[redacted] [redacted]

Copy 259
RM L56D19

NACA RM L56D19

7694

WADC
TECHNICAL LIBRARY
AFL 2811
Rq # 18454
OCT 29 1956
TECH LIBRARY KAFB, NM
0144129

NACA

RESEARCH MEMORANDUM

THE EFFECT OF EXTERNAL STIFFENING RIBS ON THE ROLLING POWER OF AILERONS ON A SWEPT WING

By Emily W. Stephens

Langley Aeronautical Laboratory
Langley Field, Va.

Classification cancelled (or changed to UNCLASSIFIED)
By Authority of NASA Tech Pub Announcement #126
(OFFICER AUTHORIZED TO CHANGE)
By ..... 2 May 58
NAME AND
GRADE OF OFFICER MAKING CHANGE)
27 Mar 61 [redacted]
[redacted]

NATIONAL ADVISORY COMMITTEE
FOR AERONAUTICS
WASHINGTON
October 25, 1956

[redacted]

[redacted]

TECH LIBRARY KAFB, NM
0144129

NATIONAL ADVISORY COMMITTEE FOR AERONAUTICS

RESEARCH MEMORANDUM

THE EFFECT OF EXTERNAL STIFFENING RIBS ON THE ROLLING POWER OF AILERONS ON A SWEPT WING

By Emily W. Stephens

SUMMARY

A limited free-flight investigation to determine some effects on rolling effectiveness and drag of external ribs, or load carrying fences, which were alined with the direction of flight, on swept wings of two different stiffnesses has been conducted by the Pilotless Aircraft Research Division of the Langley Aeronautical Laboratory. These tests showed that for the particular configuration tested, the primary effect of adding load carrying fences was structural rather than aerodynamic. It was found that adding fences to a wing which roughly simulated the stiffness characteristics of a wing of a present-day fighter airplane decreased the wing torsional flexibility by approximately 25 percent which resulted in increased zero-lift rolling effectiveness and an increase in the reversal Mach number from 0.95 to 1.01.

INTRODUCTION

In view of the trend in recent years toward increasingly thinner wings on supersonic aircraft, methods are needed for obtaining greater wing stiffness without large aerodynamic penalties. External ribs which are alined parallel to the air flow may be of appreciable value as a means of providing such additional structural stiffness for swept wings. In addition, such ribs may be quite useful in decreasing chordwise deformations on unswept wings as well.

At supersonic speeds wave drag probably is of greater importance than the drag due to skin friction, and it is believed that any drag increase resulting from the use of thin external stiffeners which are alined parallel to the air flow would arise chiefly from the increase in wetted area, provided the leading and trailing edges of the stiffeners were properly sharpened. Hence, the increased structural stiffening achieved by external ribs may more than counterbalance the drag penalty in certain applications.

It is the purpose of this paper to present the results of a limited investigation of a particular application of this stiffening method to a swept wing. Flight tests utilizing rocket-powered test vehicles in free flight were conducted by the Pilotless Aircraft Research Division to determine some effects of external ribs on rolling effectiveness and drag. The tests were made over a Mach number range of approximately 0.6 to 1.6 on wings swept 45° at the quarter chord and having aspect ratios of 4.0, taper ratios of 0.6, and NACA 65A006 airfoil sections parallel to the free stream. The controls employed were one-half-span outboard flap-type ailerons of 30 percent chord.

The configuration tested in the current program was selected because a fairly comprehensive investigation had been conducted previously on the same configuration without fences. (See ref. 1.) The spanwise spacing and dimensions of the fences were arbitrarily chosen and do not necessarily represent conditions of maximum effectiveness.

Detailed investigation into other probable useful applications of this method of stiffening wings lies beyond the scope of this paper.

SYMBOLS

b	diameter of circle swept by wing tips, 3.0 ft
c	local chord, ft
c_{av}	average exposed chord parallel to model center line, 0.72 ft
c_r	wing chord at and parallel to model center line, 0.94 ft
c_t	wing chord at tip, parallel to model center line, 0.56 ft
C_{D_T}	total drag coefficient, $\frac{\text{Drag}}{qS}$
c^4/GJ	nonscalar torsional-stiffness parameter, in.^{2}/lb
h/c	height of fence, percent local chord
i_w	average incidence per wing for three wings measured in plane normal to wing-chord plane and parallel to free stream, positive if tending to produce clockwise roll when viewed from rear, deg
m	couple, applied near wing tip in plane parallel to free stream and normal to wing-chord plane, in-lb

M	Mach number
p	rolling velocity; positive if model is rolling clockwise when viewed from rear, radians/sec
pb/2V	wing-tip helix angle or rolling-effectiveness parameter, radians
q	dynamic pressure, lb/sq ft
R	Reynolds number of tests, based on c_{av}
S	exposed area of three wings, 2.8 sq ft
t	fence thickness, in.
V	flight-path velocity, ft/sec
δ_a	deflection of one aileron measured in plane normal to wing-chord plane and perpendicular to hinge line (positive trailing edge down when wing is on left), average for three wings, deg
λ	taper ratio, $\frac{c_t}{c_r} = 0.6$
θ	angle of twist at any section along wing span in plane parallel to free stream and normal to wing-chord plane, radians
θ/m	wing-torsional-flexibility parameter associated with a twisting couple, radians/in-lb

MODELS AND TESTS

A photograph of a typical rocket-powered flight-test vehicle is shown in figure 1. Geometric and structural details of the test wings used on the flight models are presented in figure 2 and table I. The test wings had quarter-chord lines swept 45°, aspect ratios of 4.0, taper ratios of 0.6, and NACA 65A006 airfoil sections parallel to the free stream. The wings employed 30-percent-chord one-half-span outboard flap-type ailerons preset to a deflection of 10° normal to the hinge line.

The fences were made of mild steel and were 6 percent of the local chord in height; they were located at four spanwise stations. (See fig. 2.) The fences inboard of the aileron extended over the total chord, whereas the fences located in front of the aileron extended from the leading edge to the aileron hinge line.

In order to attach the stiffeners securely to the wings it was necessary to cut through the outermost fibers of the wing cross section to permit riveting of the fences to the chord-plane stiffener. (See table I.) This involved an appreciable reduction in the stiffness of the basic wing structure.

The flight tests were conducted at the Langley Pilotless Aircraft Research Station at Wallops Island, Va. The test vehicles were propelled by a two-stage rocket-propulsion system to a Mach number of about 1.6. Time-history measurements were made of the flight-path velocity with a CW Doppler radar set and of the rolling velocity with special spinsonde radio equipment. These data in conjunction with space coordinates obtained through the use of modified 584 tracking radar and atmospheric data obtained with radiosondes permit the evaluation of the rolling effectiveness parameter $pb/2V$ and the total drag coefficient C_{D_T} as functions of Mach number.

The internal structural details of the wings are shown in table I. Models A and B are identical flexible-wing models and models C and D are identical stiff-wing models, with the exception that fences have been attached to models B and D. The fences are approximately 0.03 inch thick and are located on both upper and lower surfaces of the wings. (See fig. 2.)

The Reynolds number based on average wing chord varied from approximately 2×10^6 to 8×10^6 over the Mach number range tested. (See fig. 3.) The dynamic pressures which existed for these tests are presented in figure 4.

Static tests were made to determine the wing torsional flexibility of the models. Results of these tests are presented in figure 5. Sufficient ground tests (not presented herein) were made of other wings using fences to substantiate the idea that adding fences appreciably increases the wing stiffness of swept wings, particularly in torsion.

ACCURACY AND CORRECTIONS

Based on mathematical analysis and previous experience, the maximum experimental error is estimated to be within the following limits:

	Subsonic	Supersonic
Mach number, M	±0.01	±0.01
Wing-tip helix angle, $pb/2V$, radians	±0.005	±0.003
Total drag coefficient, C_{D_T}	±0.003	±0.002

The data were corrected for effects of wing incidence by means of the equation (see ref. 2)

$$\Delta \frac{pb}{2V} = \frac{2i_w}{57.3} \frac{1 + 2\lambda}{1 + 3\lambda}$$

where $\Delta \frac{pb}{2V}$ is the increment in rolling effectiveness due to deviation in wing incidence from the nominal value of $i_w = 0^\circ$. Small differences which occurred in the aileron deflection were corrected for by assuming a linear variation of rolling effectiveness with aileron deflection and correcting to a nominal value of 10° normal to aileron hinge line. The corrections were small; $i_w = 0^\circ \pm 0.06^\circ$ and $\delta_a = 10.0^\circ \pm 0.2^\circ$.

The deviation of measured values of rolling velocity from steady-state values because of the effects of model inertia about the roll axis was estimated to be less than 1 percent (see ref. 3) and no corrections were made.

RESULTS AND DISCUSSION

Effect of Fences on Wing Stiffness

Figure 5 presents a comparison of the measured spanwise variation of the torsional-flexibility parameter θ/m for the plain wing models and the models employing load carrying fences. The data presented show the overall effect of adding the fences. In the case of the more flexible wing, the torsional flexibility was decreased approximately 20 to 25 percent by adding fences; whereas a slight increase in flexibility was measured for the stiffer wings because of practical difficulties encountered in the construction of the wings.

The overall stiffness of the flexible wing roughly approximated the stiffness of a wing used on present-day fighter airplanes. The stiff wing was approximately five times as stiff as the flexible wing tested. This wing was considered sufficiently rigid without fences, so that any changes in rolling effectiveness or drag would be due primarily to the aerodynamic effect of the fences.

Effect of Fences on Rolling Effectiveness

The rolling effectiveness of models having two different degrees of torsional flexibility, with and without fences, is presented in figure 6. Comparison of models A and B shows that adding fences to the flexible wings caused an increase in rolling effectiveness throughout the Mach

number region from approximately 0.6 to 1.6. The addition of the fences caused an increase of about 0.015 (62 percent at $M = 0.8$) in $pb/2V$ below the reversal Mach number and increased the reversal Mach number from 0.95 to 1.01.

Addition of fences to the stiffer wings (models C and D) resulted in a slightly more flexible wing for the fence model (as explained in the preceding section) and a somewhat lower rolling effectiveness.

The difference between the rolling effectiveness of models A and B and of models C and D could be closely approximated by the method of reference 4 (within the limits of applicability of the reference) when the experimental torsional flexibility values were used. It appears, therefore, that in both cases, addition of the fences had little effect on direct aerodynamics but affected the rolling power of the ailerons through an aeroelastic effect.

The Effect of Fences on Drag

Figure 7 shows that adding fences caused some increase in the total drag coefficient C_{D_T}. The drag increase was roughly 10 percent throughout the speed range tested. Figure 7 shows also that the fences caused a slight lowering of the drag-divergence Mach number.

At subsonic speeds, the measured drag increment due to the addition of fences agreed reasonably well with the estimated drag increment due to skin friction. (See ref. 5.) At supersonic speeds, skin friction accounted for approximately one-third the measured drag increment. The fences tested employed hand-sharpened leading and trailing edges (approximately 90° included angle) as a manufacturing expedient and contributed appreciable wave- and base-drag increments at the supersonic speeds tested, estimated to be approximately equal to that due to skin friction. Rough estimates were made of the drag that would be obtained by using sharpened fences (20° included angle). At supersonic speeds, the drag due to skin friction would be approximately the same as for the fences used in this report; however, the pressure drag would be only one-half that contributed by the fences having 90° included angle.

Tests were conducted in the Langley 16-foot transonic tunnel on a model with chordwise fences which had the same wing configuration as the models of the current investigation but a different body shape. Results of these tests showed that the addition of fences had little aerodynamic effect except to increase the drag coefficient for zero-lift conditions by approximately 15 percent over the Mach number range from 0.90 to 1.03. This increase was of the same order of magnitude as the increase in drag coefficient obtained when fences were added to the models discussed in this paper.

CONCLUSIONS

A limited free-flight investigation has been conducted to determine some effects on rolling effectiveness and drag of external ribs, or fences, which were alined with the direction of flight, on wings swept 45° at the quarter chord and having taper ratios of 0.6, aspect ratios of 4.0, NACA 65A006 airfoil sections parallel to the free stream and one-half-span outboard flap-type ailerons of 30 percent chord. The following conclusions are indicated:

1. The primary effect of adding fences to a swept wing is to decrease the torsional flexibility. These tests show that adding fences decreased the wing torsional flexibility by approximately 20 to 25 percent, which resulted in an increase of about 0.015 (62 percent at a Mach number of 0.8) in zero-lift rolling effectiveness below the reversal Mach number and an increase in the reversal Mach number from 0.95 to 1.01.

2. As far as could be determined, the aerodynamic effects on zero-lift rolling effectiveness due to adding fences are negligible, although the total drag coefficient was increased approximately 10 percent throughout the Mach number region from approximately 0.6 to 1.6.

Langley Aeronautical Laboratory,
National Advisory Committee for Aeronautics,
Langley Field, Va., April 3, 1956.

REFERENCES

1. Schult, Eugene D., Strass, H. Kurt, and Fields, E. M.: Free-Flight Measurements of Some Effects of Aileron Span, Chord, and Deflection and of Wing Flexibility on the Rolling Effectiveness of Ailerons on Sweptback Wings at Mach Numbers Between 0.8 and 1.6. NACA RM L51K16, 1952.

2. Strass, H. Kurt, and Marley, Edward T.: Rolling Effectiveness of All-Movable Wings at Small Angles of Incidence at Mach Numbers From 0.6 to 1.6. NACA RM L51H03, 1951.

3. Sandahl, Carl A., and Marino, Alfred A.: Free-Flight Investigation of Control Effectiveness of Full-Span 0.2-Chord Plain Ailerons at High Subsonic, Transonic, and Supersonic Speeds To Determine Some Effects of Section Thickness and Wing Sweepback. NACA RM L7D02, 1947.

4. Strass, H. Kurt, and Stephens, Emily W.: An Engineering Method for the Determination of Aeroelastic Effects Upon the Rolling Effectiveness of Ailerons on Swept Wings. NACA RM L53H14, 1953.

5. Van Driest, E. R.: The Turbulent Boundary Layer for Compressible Fluids on a Flat Plate With Heat Transfer. Rep. No. AL-997, North American Aviation, Inc., Jan. 27, 1950.

TABLE I

INTERNAL CONSTRUCTION DETAILS

	Model	Surface inlay	Center-line stiffener	Fences		Ref.
				h/c	t, in.	
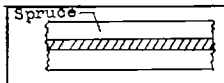	A	—	0.125" aluminum alloy	—	—	1
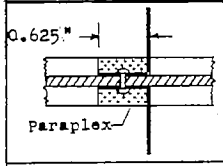	B	—	↓	.06	.03	—
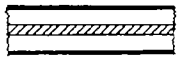	C	0.04" steel (0.15c to 0.70c)	↓	—	—	1
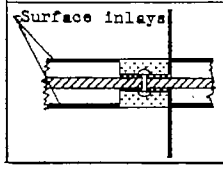	D	↓	↓	.06	.03	—

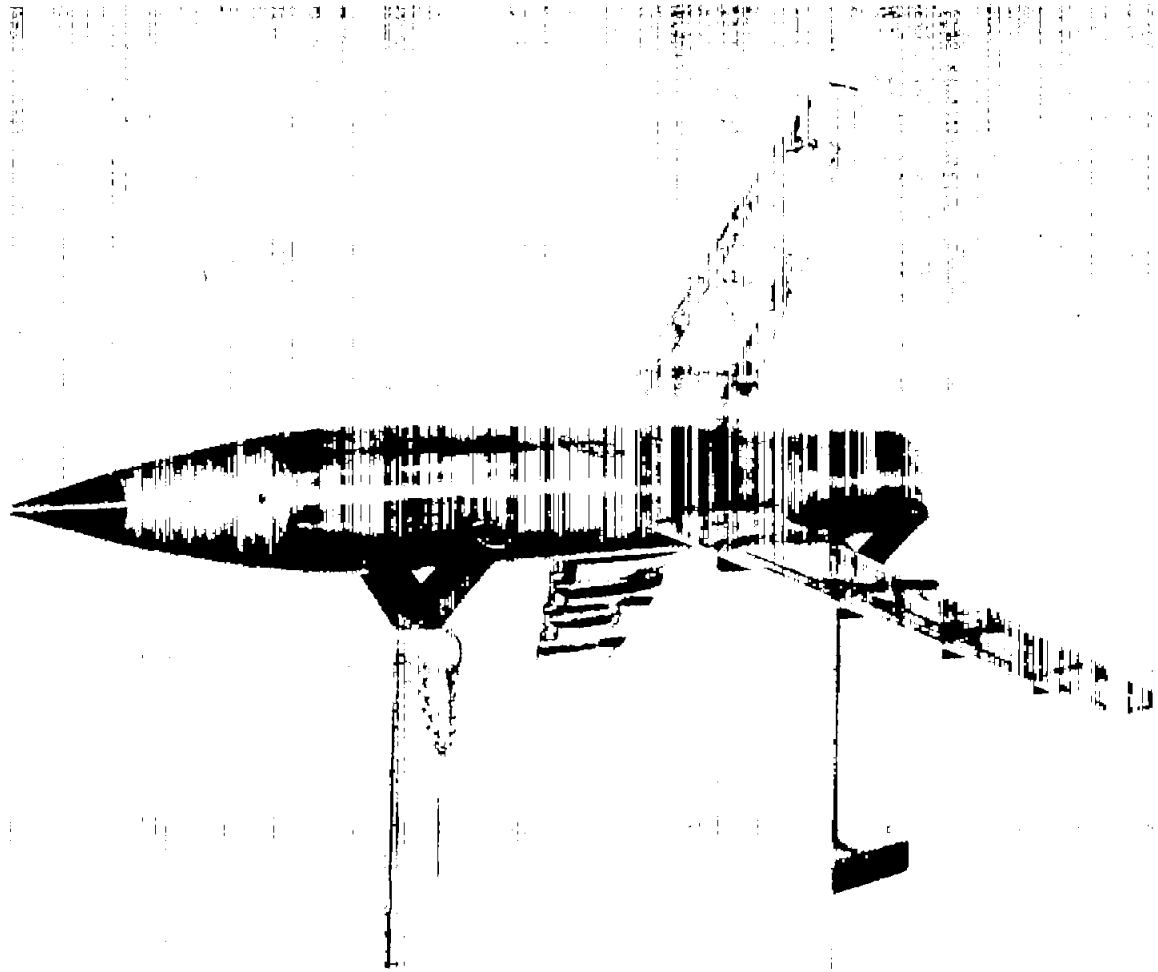

L-89286.1

Figure 1.- Oblique view of a typical rocket-powered test vehicle.

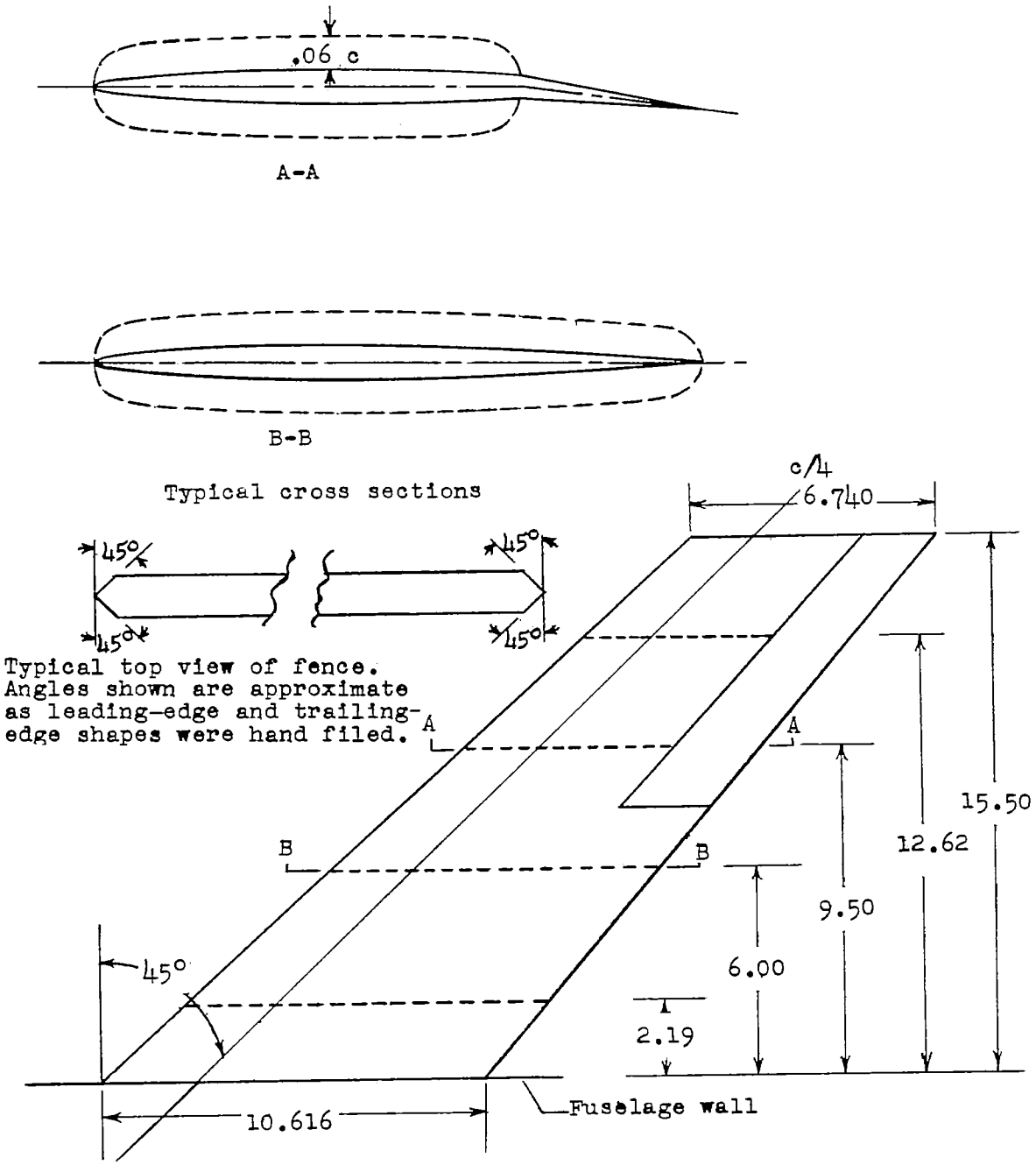

Figure 2.- External characteristics of a typical test wing showing location of fences. All dimensions are in inches unless otherwise noted.

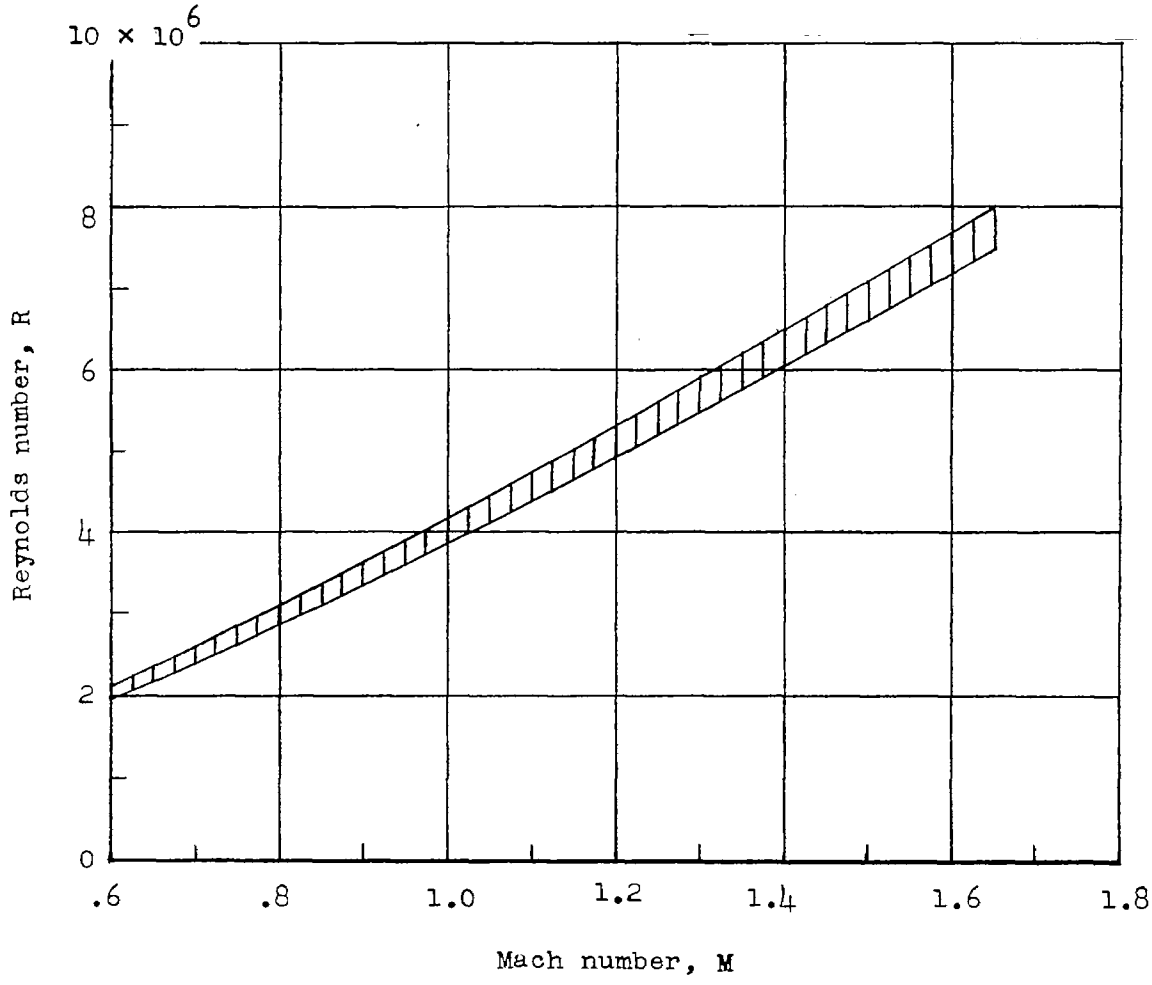

Figure 3.- Reynolds number based on average wing chord plotted against Mach number for all tests.

[redacted]

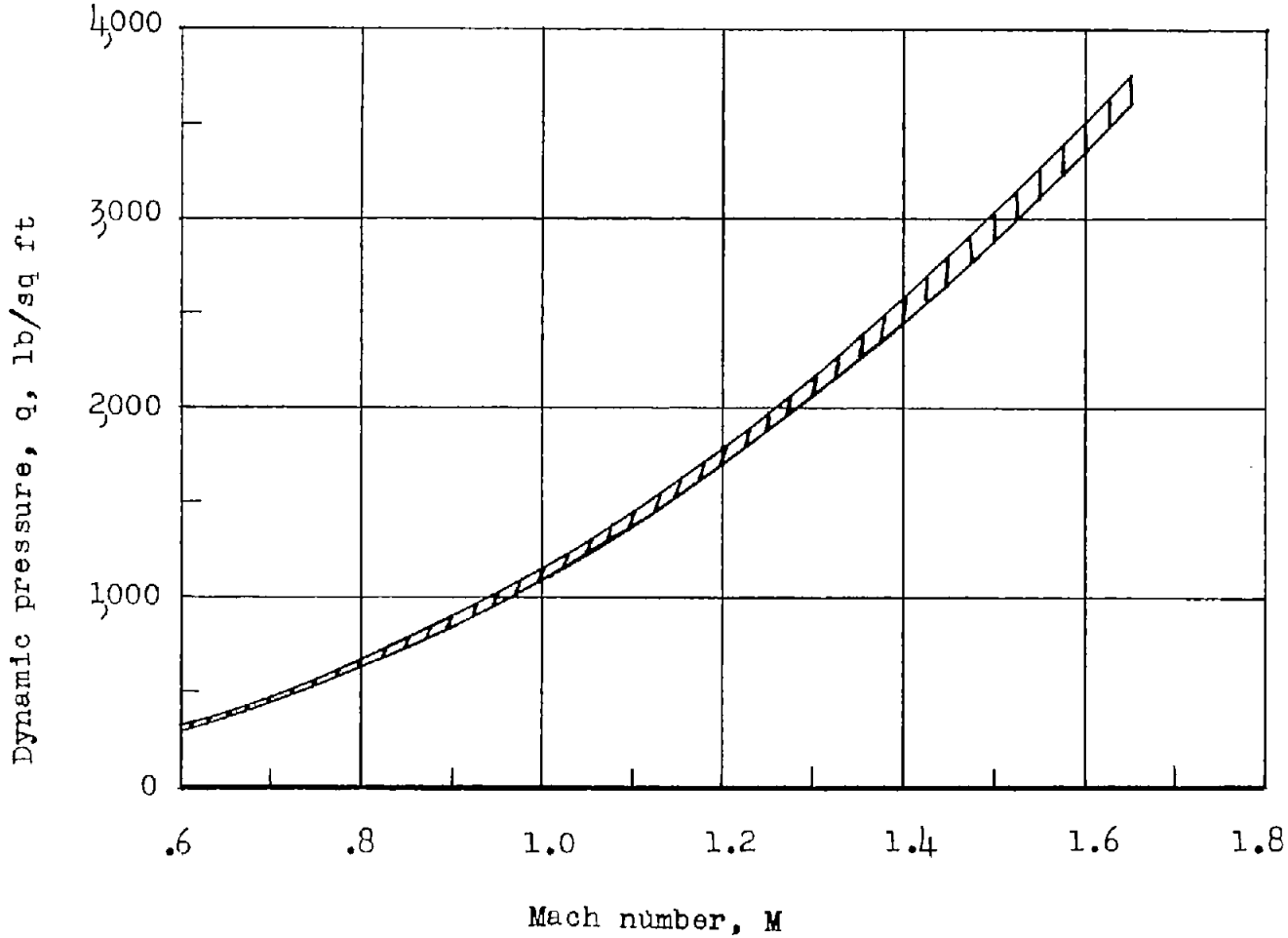

Figure 4.- Dynamic pressure plotted against Mach number for all tests.

[redacted]

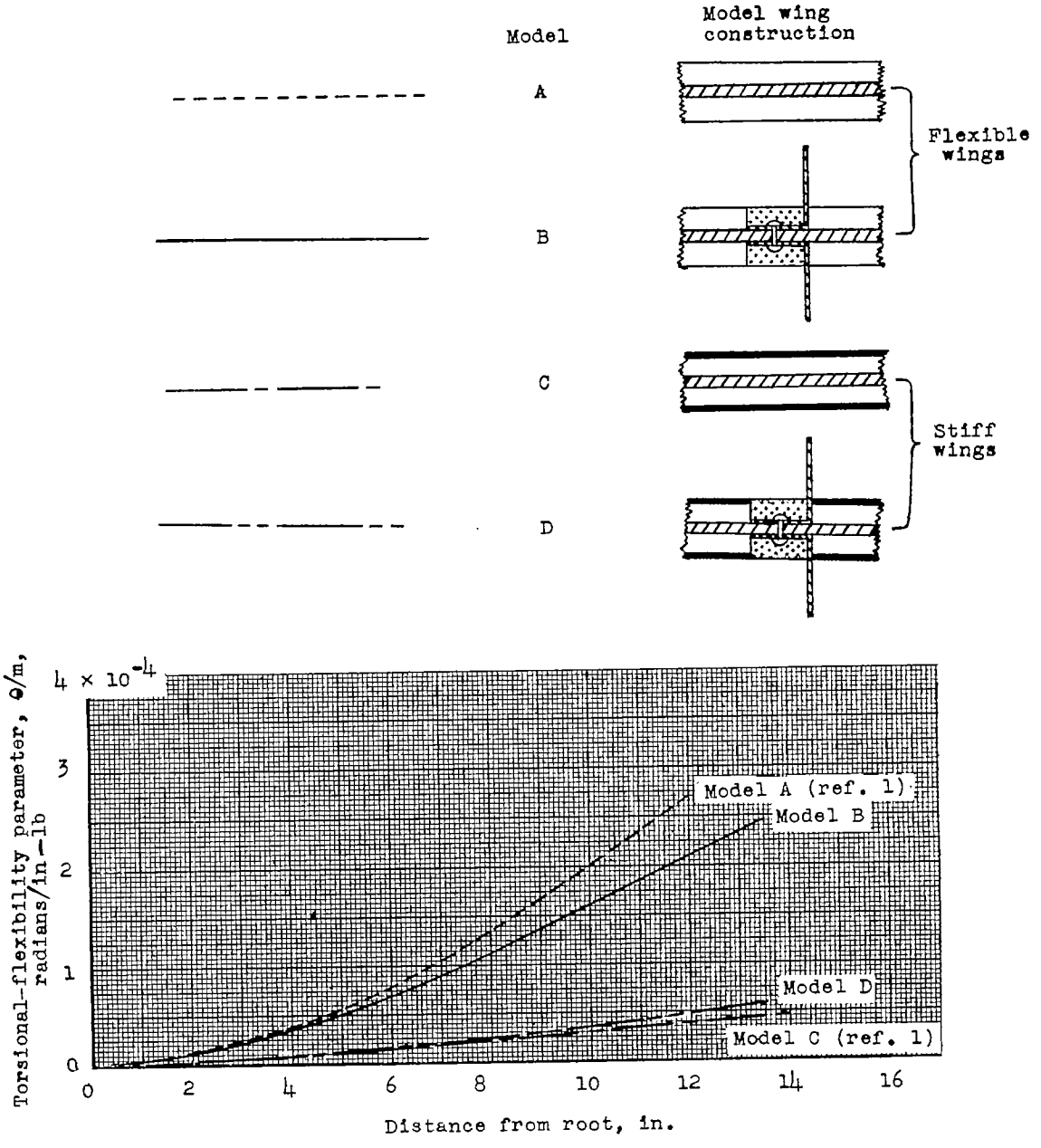

Figure 5.- Variation of wing torsional-flexibility parameter with wing semispan. Couple applied at wing tip in a plane normal to wing-chord plane and parallel to body axis.

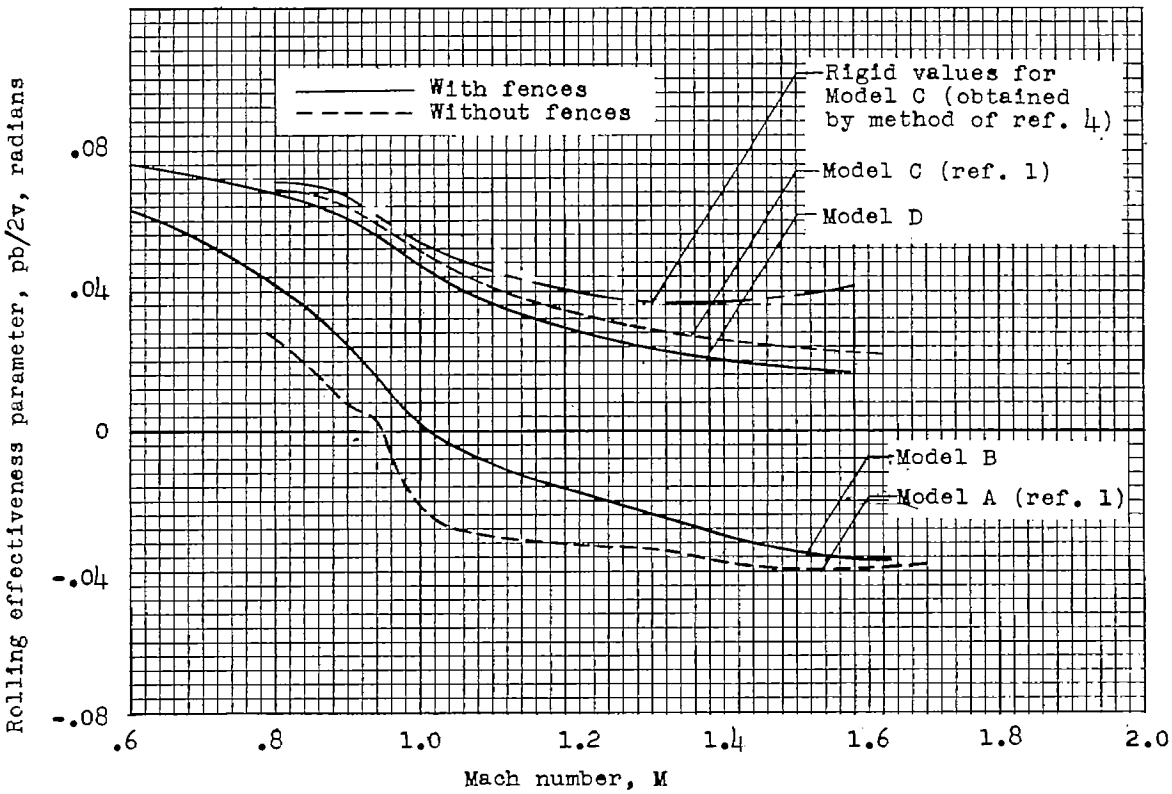

Figure 6.- Rolling effectiveness parameter plotted against Mach number; $i_W = 0^{\circ}$; $\delta_a = 10.0^{\circ}$ normal to hinge line.

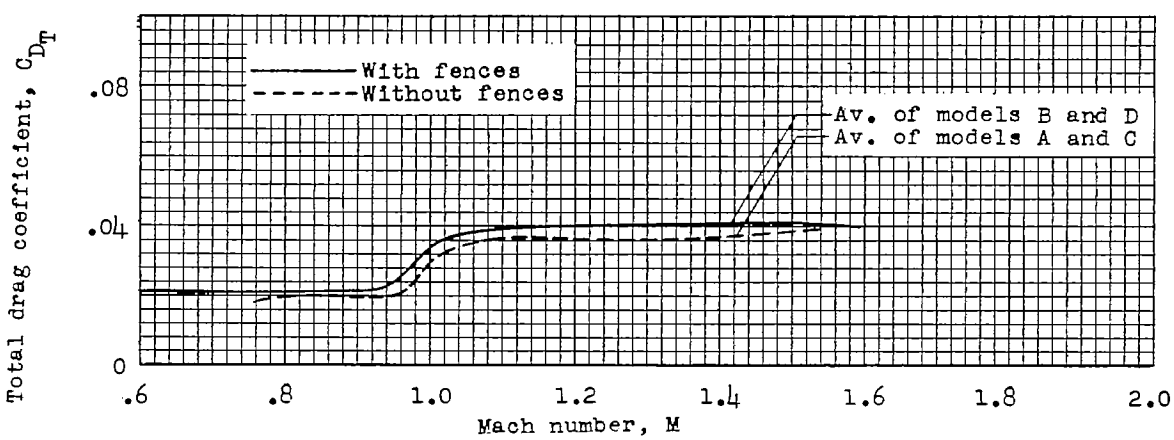

Figure 7.- Total drag coefficient plotted against Mach number.

NACA - Langley Field, Va.

[redacted]